Analysis of pressure and pressure derivative interference tests under linear and spherical flow conditions

Freddy Humberto Escobar-Macualo, Esteban Rojas-Borrego & Neila Tatiana Alarcón-Olaya

Grupo de Investigación GIPE de la Facultad de Ingeniería, Universidad Surcolombiana, Neiva, Colombia. fescobar@usco.edu.co, rojasborrego@gmail.com, ntalarcon123@gmail.com

Abstract
Often, interpretation of interference tests is performed for systems acting under radial flow regimen conditions by means of conventional straight-line method, type-curve matching and *TDS* technique. For linear and spherical flow cases, the interpretation of interference tests is performed by the conventional analysis and type-curve matching. These procedures do not allow verification of the estimated parameters; therefore, this paper presents the formulation of a more practical, useful and accurate methodology which is achieved based upon the determination of characteristic features found on the pressure and pressure derivative versus time log-log plot with the purpose of developing analytical expressions for the interpretation of interference tests under spherical and linear flow conditions. These equations were successfully verified by their application on synthetic tests.

Keywords: interference testing; linear flow; spherical flow; steady state; pseudosteady state.

Análisis de presión y derivada de presión en pruebas de interferencia en condiciones de flujos lineal y esférico

Resumen
Normalmente, la interpretación de las pruebas de interferencia se realiza en sistemas que actúan bajo condiciones de régimen flujo radial utilizando análisis convencional de la línea recta, curvas tipo y técnica *TDS*. Para los casos de flujos lineal y esférico, la interpretación de pruebas de interferencia se realiza mediante el método convencional y el ajuste con curvas tipo. Estos procedimientos no permiten verificación de los parámetros estimados, y por ello en este trabajo se presenta una formulación de una metodología más práctica, útil y práctica mediante el uso de rasgos característicos en el gráfico logarítmico de la presión y derivada de presión contra tiempo, que permitan desarrollar expresiones analíticas directas usadas para la caracterización del yacimiento en pruebas interferencia en condiciones de flujos esférico y lineal. Estas ecuaciones se verificaron satisfactoriamente mediante a su aplicación a pruebas sintéticas.

Palabras clave: pruebas de interferencia; flujo lineal; flujo esférico; estado estable; estado pseudoestable.

1. Introducción

Normally, the methods used for interference tests interpretation are type-curve matching and the conventional straight-line method. In the study by [11] on water flow in aquifers and its influence on water-producing wells, he took the first steps in developing a graphical analysis method that intermediate the field data and the theoretical data for radial regime, which is known as type-curve matching method. Later [2,12,15,18], among others, improved this form of analysis for interference tests by involving either conventional analysis or the pressure derivative function. Type-curve matching is not only tedious but highly inaccurate with a slight data point reading variation.

The first application of the pressure derivative in interference tests was done by [18]. This method did not have much impact at first because it made use of the arithmetic derivative and secondly the noise introduced to the pressure data by external sources increased with the derivative and before the 90s there was not many studies with the estimate

of the pressure derivative function. A subsequent analysis was performed by [5], taking as reference the work done by [18] for two-rate testing.

[13] presented the analytical models for radial, linear and spherical flow regimes and used type-curve matching and regression analysis for the interpretation of interference tests. In addition to presenting the analytical interference solution for radial flow regime, [13] also presented the solutions for linear and spherical flow regimes. The first one occurs in elongated deposits caused by channeling or faulting and the second one in very thick formations. [17] followed the philosophy of the *TDS* Technique, [19], for interference testing using the intersection between pressure and pressure derivative. Later, these recently mentioned works were applied by [7] to determine heterogeneities from interference testing. *TDS* Technique has many applications, just to name a few of them, [6] and [8] extended this methodology for interpreting pressure tests in elongated systems, and [14] developed the *TDS* for heavy oil obeying power-law behavior. Much more applications of the *TDS* Technique were compiled by [9].

Formulating a more practical interpretation methodology for interpretation of interference tests under linear and spherical conditions is the purpose of this paper. For this, the starting points are the linear and spherical solutions presented by [13] so the behavior of pressure and the pressure derivative curves are generated, and, from observations at characteristic points analytical expressions are developed to allow interpreting interference tests in a simple, practical and accurate way. Additionally, based on the work of [3,10], the presence of either pseudosteady-state or steady-state periods was used to develop expressions for the determination of the well drainage area when the duration of the test allows it. The expressions developed were verified satisfactorily with their application to synthetic tests.

2. Mathematical model

For the development of the TDS Technique, [19], in interference tests where either linear or spherical conditions are presented, it is necessary to understand the pressure and pressure derivative behavior in each system with the purpose of finding special features or straight lines which allow obtaining mathematical expressions for reservoir characterization.

2.1. Lineal flow regime model

[16] presented the solution for the pressure distribution in linear systems. This solution was considered for the case of a well producing a constant flow and infinite system. In addition, for an interference test, it was assumed that only half of the active well flow rate is perceived in the observer well. The pressure drop for the described condition is:

$$\Delta P_L = 2\pi\alpha_L \frac{qB\mu}{kbh} \left\{ \sqrt{\frac{4\beta\eta t_L}{\pi}} \exp\left(-\frac{x^2}{4\beta\eta t_L}\right) - x\,erfc\left(\sqrt{\frac{x^2}{4\beta\eta t_L}}\right) \right\} \tag{1}$$

And the pressure derivative is given by:

$$(t*\Delta P')_L = 2\pi\alpha_L \frac{qB\mu}{kbh} \sqrt{\frac{\beta\eta t_L}{\pi}} \exp\left(\frac{-x^2}{4\beta\eta t_L}\right) \tag{2}$$

The dimensionless parameters are given as:

$$t_D = \frac{0.0002637kt}{\phi\mu c_t r_w^2} \tag{3}$$

$$P_D = \frac{kh\Delta P}{141.2q\mu B} \tag{4}$$

$$t_D * P_D' = \frac{kh(t*\Delta P')}{141.2q\mu B} \tag{5}$$

Eqs. (1) and (2) allowed generating several pressure and pressure curves as given in Fig. 1 using data from Table 1. As either the reservoir width, *b*, or the distance between the wells, *L*, or the reservoir thickness, *h*, varies so do the pressure and pressure derivative curves; therefore, a unique behavior was obtained after multiplying both dimensionless pressure and pressure derivative and dimensionless time values by certain parameters as shown in Fig. 2. Notice in Eq. (3) that the squared wellbore radius can be changed by drainage area obtained the dimensionless time based on area, t_{DA}.

From the unified behavior observed in Fig. 2, a unique intersection point with coordinates 270869.0956, 0.1006 is found:

Table 1.
Input data for generating data in Figure 1.

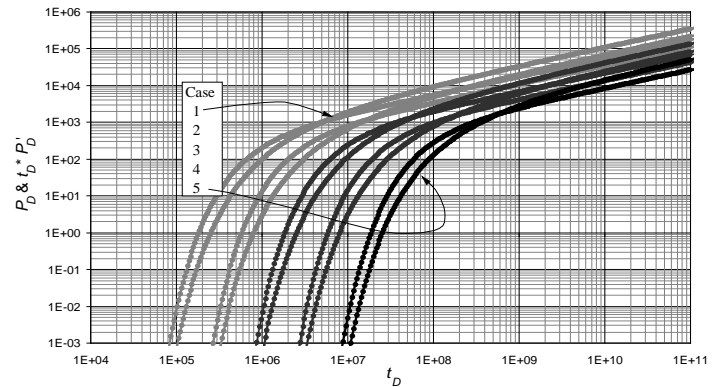|	Case 1	Case 2	Case 3	Case 4	Case 5
h, ft	30	45	68	101	152
b, ft	20	32	51	82	131
L, ft	300	450	675	1013	1519
x, ft	1000	1800	3240	5832	10498

Source: The authors

Figure 1. Dimensionless pressure and pressure derivative behavior for interference tests under linear flow conditions
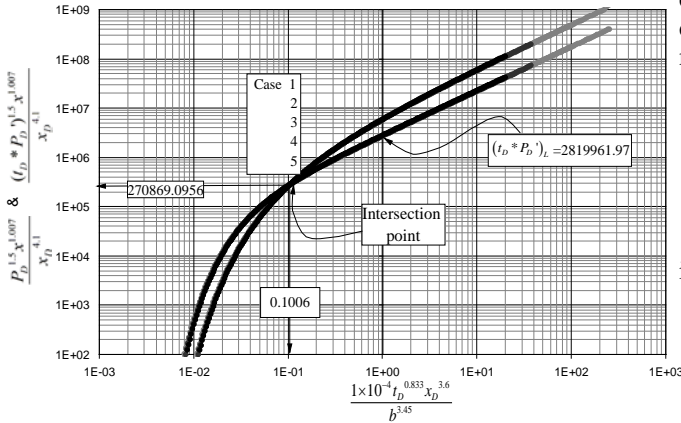Source: The authors

Figure 2. Unified pressure derivative behavior interference tests under linear flow conditions
Source: The authors

$$\frac{1 \times 10^{-4} \ t_{DL}^{0.833} x_D^{3.6}}{b^{3.45}} = 0.1006 \qquad (6)$$

After replacing the dimensionless time and the definition of dimensionless length, $x_D = x/L$, in Eq. (6), an expression to find porosity was obtained:

$$\phi = \frac{k t_{Li}}{15239024 \ \mu c_t r_w^2} \left(\frac{x}{L}\right)^{4.32} \frac{1}{b^{4.14}} \qquad (7)$$

The abscise value was:

$$\frac{P_{DL}^{1.5} x^{1.007}}{x_D^{4.1}} = 270869.0956 \qquad (8)$$

From which permeability is solved for once Eq. (4) and x_D, are replaced in the above expression:

$$k = \frac{591118.21 \ q \mu B x^{2.0620}}{h \Delta P_{Li} L^{2.7333}} \qquad (9)$$

Since the pressure and pressure derivative values are the same, Eq. (9) can also use the pressure derivative value, instead.

The governing equation for the unique linear flow regime was obtained by regression analysis to be:

$$\frac{(t_D * P_D')_L^{1.5} \ x^{1.007}}{x_D^{4.1}} = 2819961.97 \left(\frac{1 \times 10^{-4} \ t_{DL}^{0.833} x_D^{3.6}}{b^{3.45}}\right)^{0.5} \qquad (10)$$

Replacing the dimensionless parameters in Eq. (10) is possible to obtain an expression to find permeability using an arbitrary point during linear flow regime:

$$k = 510255 \left(\frac{qB}{h(t * \Delta P')_L}\right)^{1.3844} \left(\frac{t_L}{\phi c_t r_w^2}\right)^{0.3844} \frac{x^{4.5159} \mu}{L^{5.4453} b^{1.5921}} \qquad (11)$$

Because of the noise introduced to the pressure readings from

external sources, it is recommended to read the pressure derivative value during linear flow at a time, $t = 1$ hr, to obtain a more representative reading value, then, Equation (11) becomes:

$$k = 510255 \left(\frac{qB}{h(t * \Delta P')_{L1}}\right)^{1.3844} \left(\frac{1}{\phi c_t r_w^2}\right)^{0.3844} \frac{x^{4.5159} \mu}{L^{5.4453} b^{1.5921}} \qquad (12)$$

The dimensionless pressure governing was found by integration of Eq. (10); therefore:

$$P_{DL1} = \frac{3338.41 \ x^{3.2608}}{b^{1.1498} \ L^{3.9321}} t_{DL}^{0.2776} + s_L \qquad (13)$$

Dividing Eq. (13) by Eq. (10), and solving for the linear skin factor and replacing the dimensionless quantities, it yields:

$$s_L = \left(\frac{0.0002637 k t_L}{\phi \mu c_t r_w^2}\right)^{0.2776} \left(\frac{\Delta P_L \delta}{(t_D * P_D')_L} - \sigma\right) \qquad (14)$$

2.2. Spherical flow regime model

The governing pressure drop equation for a well producing a constant flow was given by [4] when spherical flow is developed in a reservoir is given by:

$$\Delta P_{sph} = \alpha_{sph} \frac{qB\mu}{2kr} erfc\left(\sqrt{\frac{\phi \mu c_t r^2}{4\beta k t_{sph}}}\right) \qquad (15)$$

Its pressure derivative is then:

$$(t * \Delta P')_{sph} = -\alpha_{sph} \frac{qB\mu}{2kr} \sqrt{\frac{\phi \mu c_t r^2}{4\beta k t_{sph}}} \exp\left(\frac{-\phi \mu c_t r^2}{4\beta k t_{sph}}\right) \qquad (16)$$

As for the former case, pressure and pressure derivative curves were generated, for this case with data from Table 2, considering the variation of wellbore radius, r_w, reservoir thickness, h, and distance between wells, r. Such curves are reported in Fig. 3.

It was also necessary to unify the pressure derivative curves to obtain a universal behavior. It was performed by multiplying both dimensionless pressure, pressure derivative and time for certain factors as shown in Fig. 4.

From the unified behavior observed in Fig. 4 a unique intersection point with coordinates 0.029163, 0.17513 is found. Therefore,

Table 2.
Input data for generating data in Figure 3.

	Case 1	Case 2	Case 3	Case 4
r_w, ft	0.3	0.45	0.5	0.54
h, ft	2000	5000	1000	700
r, ft	500	1000	300	250

Source: The authors

$$\frac{t_{Dsph} \ h_D^{0.5}}{r_D^{2.7}} = 0.17513 \qquad (17)$$

From which porosity is obtained once the dimensionless quantities are used:

$$\phi = \frac{1.5 \times 10^{-3} \, k t_{sphi} h^{0.5} r_w^{0.2}}{\mu c_t r^{2.7}} \qquad (18)$$

and;

$$\frac{P_{Dsph}}{r_D^{0.3}} = 2.9163 \times 10^{-2} \qquad (19)$$

After replacing Eq. (4), the definition of dimensionless radius and solving for the formation permeability, it yields.

$$k = \frac{4.1178 \, q\mu B}{h \, \Delta P_{sph\,i}} \left(\frac{r}{r_w} \right)^{0.3} \qquad (20)$$

Since the pressure and pressure derivative values are the same, Eq. (20) can use the pressure derivative value, instead.

The governing universal equation for spherical flow was obtained by linear regression to be:

$$\frac{(t_D * P_D{}')_{sph}}{r_D^{0.3}} = 2.17 \times 10^{-2} \left[\frac{t_{Dsph} h_D^{0.5}}{r_D^{2.7}} \right]^{-0.5} \qquad (21)$$

Replacing the dimensionless parameters in Eq. (21), it is possible to obtain an expression to find permeability using an arbitrary point during linear flow regime:

$$k = \frac{32.8972 \mu r^{1.1}}{r_w^{0.2667} h^{0.8334}} \left(\frac{\phi c_t}{t_{sph}} \right)^{0.3333} \left(\frac{qB}{(t * \Delta P{}')_{sph}} \right)^{0.6667} \qquad (22)$$

As for the linear case, because of the noise, it is recommended to apply Eq. (22) at the time of 1 hr.

The dimensionless pressure governing equation was obtained by integration of Eq. (25), to be:

$$P_{Dsph1} = \frac{-4.34 \times 10^{-2} \, r^{3.3}}{r_w^{2.8} h^{0.5}} t_{Dsph}^{-0.5} + s_{sph} \qquad (23)$$
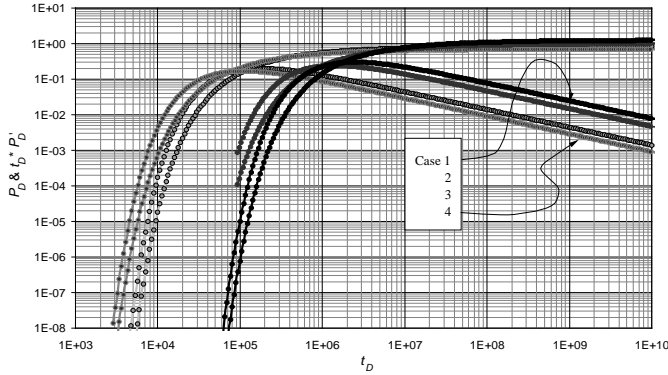

Figure 3. Dimensionless pressure and pressure derivative behavior for interference tests under spherical flow conditions
Source: The authors

Figure 4. Unified pressure derivative behavior interference tests under spherical flow conditions
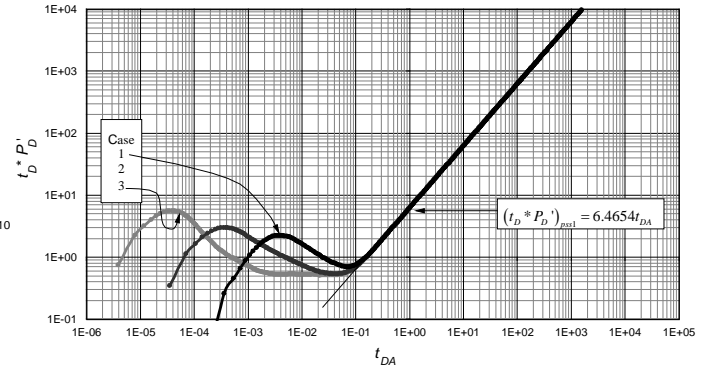Source: The authors

Figure 5. Dimensionless pressure behavior versus dimensionless time based on area for spherical flow interference in closed systems
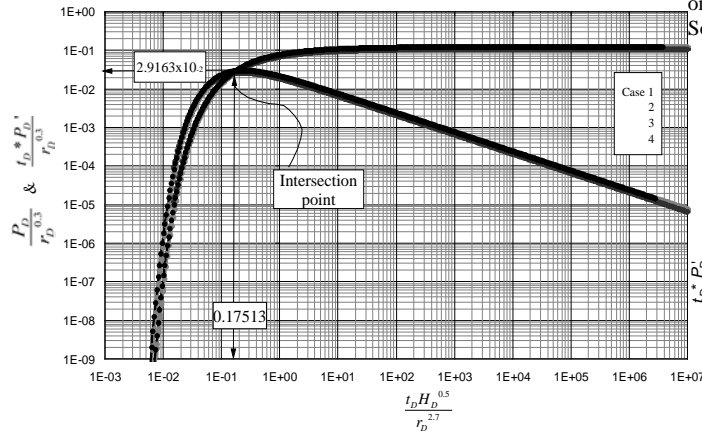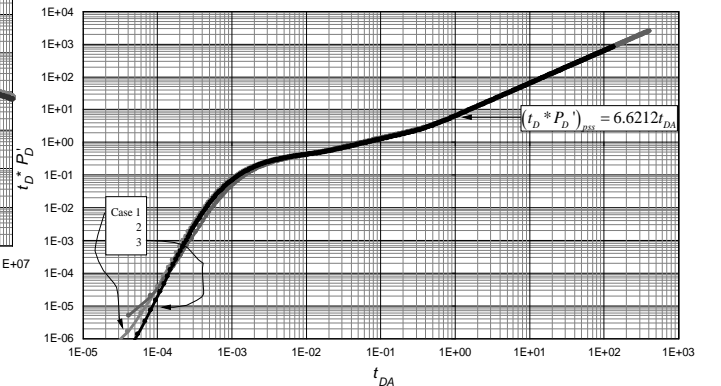Source: The authors

Figure 6. Dimensionless pressure behavior versus dimensionless time based on area for linear flow interference in closed systems
Source: The authors

Dividing Eq. (23) by Eq. (21), replacing the dimensionless quantities and solving for the spherical skin factor will result:

$$s_{sph} = \left(\frac{0.0002637 k t_{sph}}{\phi \mu c_t r_w^2} \right)^{-0.5} \left(\frac{\Delta P_{sph} \delta}{(t * P\,')_{sph}} - \sigma \right) \qquad (24)$$

2.3. Late time behavior

The basis for interference in bounded systems were given by [3]. The application of the pressure derivative for limited reservoirs was presented by [10]. This means that it is feasible to develop either pseudosteady-state or steady-state periods during an interference test. As observed in Fig. 5, once spherical flow regime vanishes pseudosteady-state period obeys the following governing pressure derivative equation:

$$(t_D * P_D\,')_{pss} = 6.4654 t_{DA} \qquad (25)$$

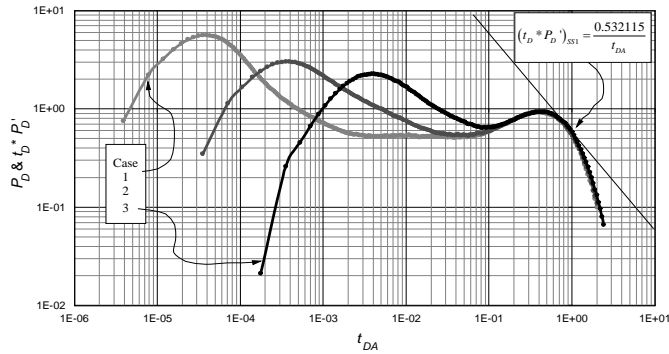Replacing the dimensionless quantities and solving for the drainage area, it results:

Figure 7. Dimensionless pressure behavior versus dimensionless time based on area for spherical flow interference in constant-pressure systems
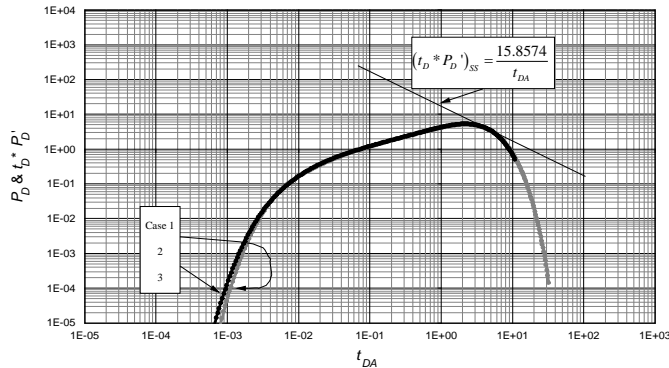Source: The authors

Figure 8. Dimensionless pressure behavior versus dimensionless time based on area for linear flow interference in constant-pressure systems
Source: The authors

$$A = \frac{0.2407 q B t_{pss}}{\phi c_t h (t * \Delta P\,')_{pss}} \qquad (26)$$

As shown in Fig. 6 the pressure derivative governing equation is given by:

$$(t_D * P_D\,')_{pss} = 6.6212 t_{DA} \qquad (27)$$

As for the spherical flow case, after replacing the dimensionless time based on area, the resulting area equation was:

$$A = \frac{0.2465 q B t_{pss}}{\phi c_t h (t * \Delta P\,')_{pss}} \qquad (28)$$

On the other hand, for constant-pressure bounded systems, Figs. 7 and 8, the late-time governing pressure derivative equations for linear and spherical flow regimes, respectively are given by:

$$\left(t_D * P_D\,'\right)_{SS} = \frac{0.532115}{t_{DA}} \qquad (29)$$

Replacing the dimensionless quantities and solving for the drainage area results in:

$$A = \frac{3.5087 \times 10^{-6} k^2 h t_{SS} (t * \Delta P\,')_{SS}}{q \mu^2 \phi c_t B} \qquad (30)$$

As shown in Fig. 8 the pressure derivative governing equation is given by:

$$\left(t_D * P_D\,'\right)_{SS} = \frac{15.8574}{t_{DA}} \qquad (31)$$

Replacing the dimensionless quantities and solving for the drainage area, it results:

$$A = \frac{0.011778 k^2 h t_{SS} (t * \Delta P\,')_{SS}}{q \mu^2 \phi c_t B} \qquad (32)$$

Because of the noise, it is recommended to apply Eqs. (28), (30) and (32) at time of 1 hr.

The spherical system can be readily converted to hemispherical system. As seen in Eq. (15), the constant α_{sp} has the value of 70.6. For hemispherical flow conditions this constant is multiplied by two, taking the value of 141.2, so do the constants in the related equations. Apart from this, appendix A presents the gas flow equations for linear and spherical flow conditions.

3. Examples

Two synthetic examples were generated to validate the porosity and permeability equations and two other tests were synthetically created two verify the equations of area. Table 3 contains the input data for the examples.

Table 3.
Input data for the examples

Parameter	Example 1	Example 2	Example 3	Example 4
c_t,1/psi	1.5×10^{-6}	1.1×10^{-6}	3×10^{-5}	3×10^{-6}
k, md	240	330	400	250
ϕ	0.16	0.22	0.1	0.1
q, BPD	320	440	100	100
B, rb/STB	1.15	1.21	1.0	1.0
μ, cp	4	5.5	2	1
r_w, ft	0.4	0.5	3.54	3.6
h, ft	36	5500	6000	20
b, ft	26	1100		
L, ft	360			
x, ft	1440			
A, ft^2			1×10^8	54×10^8

Source: The authors

3.1. Example 1 (Linear)

The simulated data provided in Fig. 9 was generated with data from Table 3, from where the following information was read:

$t_{Li} = 45.71$ hr $\qquad \Delta P_{Li} = 31399.66$ psi

$t_L = 3408$ hr $\qquad (t^*\Delta P')_L = 313006.65$ psi

Then, permeability was estimated with Eqs. (9) and (11) and porosity with Eq. (7). Results are reported in Table 4.

3.2. Example 2 (spherical)

Fig. 10 presents the pressure and pressure derivative data for a synthetic test under spherical flow interference conditions which used input data from Table 3. The following information was read from such plot:

Table 4.
Results for worked examples

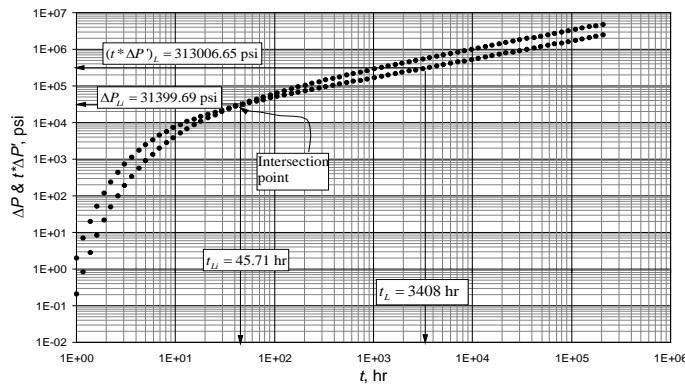| Parameter	Equation	result	% Error
		Example 1	
k, md	9	258.03	6.99
k, md	11	255.49	6.06
ϕ	7	0.1720	6.99
		Example 2	
k, md	20	352.21	6.31
k, md	22	337.91	2.34
ϕ, %	18	0.2137	2.92
		Example 3	
A, ft^2	30	101050560	1.05
		Example 4	
A, ft^2	28	5477777778	1.42

Source: The authors

Figure 9. Log-log of pressure and pressure derivative versus time for example 1 (linear case)
Source: The authors

Figure 11. Log-log of pressure and pressure derivative versus time for example 3 (spherical case)
Source: The authors

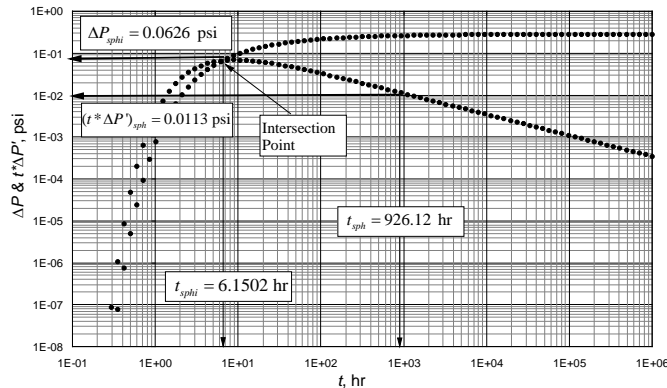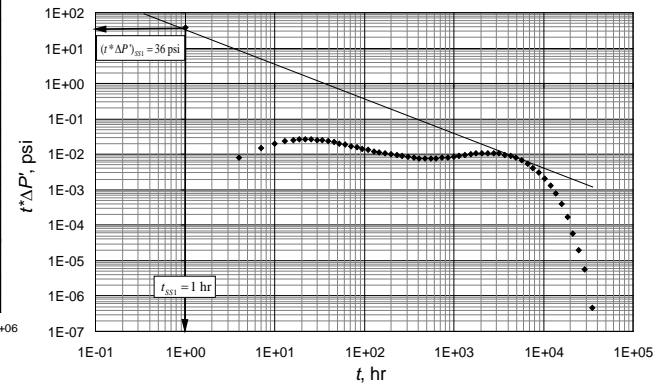Figure 10. Log-log of pressure and pressure derivative versus time for example 2 (spherical case)
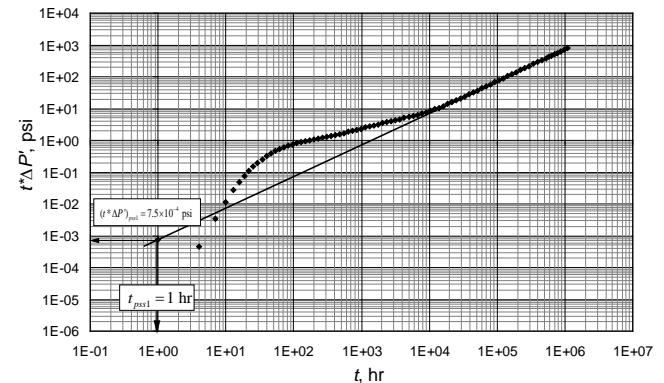Source: The authors

Figure 12. Log-log of pressure and pressure derivative versus time for example 4 (linear case)
Source: The authors

$t_{sphi} = 6.1502$ hr $\qquad \Delta P_{sphi} = 0.0626$ psi

$t_{sph} = 926.12$ hr $\qquad (t*\Delta P')_{sph} = 313006.65$ psi

Permeability was estimated using Eqs. (20) and (22). Porosity was found with Eq. (18). Results are also reported in Table 4.

3.3. Example 3 (spherical case)

A long pressure test was also simulated with input data from Table 3. The pressure and pressure derivative for this example is reported in Fig. 11 from where the following characteristic point was read:

$(t*\Delta P')_{ss1} = 36$ psi

Drainage area was estimated with Eq. (30) -reading at $t = 1$ hr- and reported in Table 4.

3.4. Example 4 (linear case)

The pressure and pressure derivative versus time data reported in Fig. 12 was also obtained using data from Table 3. The following datum was read from this figure.

$(t*\Delta P')_{pss1} = 0.00075$ psi

Drainage area was estimated with Eq. (28) -reading at $t = 1$ hr- and also reported in Table 4.

4. Conclusions

1. The intersection point, a characteristic one-half slope (for linear flow) and negative one-half slope (for spherical) flow, a late time unit-slope line (pseudosteady state) and a late time negative unit-slope line (steady state) are identified and set as characteristic features on the pressure and pressure derivative versus time log-log plot which allow developing expressions for reservoir characterization.
2. *TDS* Technique is applied to interference testing under linear and spherical flow regime conditions. A unique point of intersection - found for each case – is used to find expressions to find reservoir permeability and porosity. Also, the permeability value is verified by another expression that uses an arbitrary point read on each flow regime (linear or spherical). There are also developed equations to estimate the drainage area in both dealt flow regimes for close or constant-pressure boundary systems. The Equations are successfully verified on synthetic cases.

References

[1]   Agarwal, R.G., Real gas pseudo-time - A new function for pressure buildup analysis of MHF gas wells. Society of Petroleum Engineers. January 1. 1979, DOI: 10.2118/8279-MS.

[2]   Al-Marhoun, M.A., Interference testing: A new analysis approach. Society of Petroleum Engineers, 1985. DOI: 10.2118/13732-MS.

[3]   Brown, M.W. and Ambastha, A.K., Interference test analysis for rectangular reservoirs. Petroleum Society of Canada. January 1. 1991, DOI: 10.2118/91-45.

[4]   Chatas, A.T. Unsteady spherical flow in petroleum reservoir. SPE J. 6(2), pp. 102-114; 1966. Trans., AIME, 237. SPE-1305-PA. DOI: 10.2118/1305-PA.

[5]   El-Khatib, N.A.F., A new approach to interference test. SPE Formation Evaluation, 2(4): pp. 609-610. 1987. Society of Petroleum Engineers. DOI: 10.2118/13733-MS.

[6]   Escobar, F.H., Hernández, Y.A. and Hernández, C.M., Pressure transient analysis for long homogeneous reservoirs using TDS technique. Journal of Petroleum Science and Engineering. 58(1-2), pp. 68-82, 2007. DOI: 10.1016/j.petrol.2006.11.010.

[7]   Escobar, F.H., Cubillos, J., Montealegre-M., M., Estimation of horizontal reservoir anisotropy without type-curve matching. Journal of Petroleum Science and Engineering 60, pp. 31-38. 2008. DOI: 10.1016/j.petrol.2007.05.003.

[8]   Escobar, F.H., Montealegre-M., M. and Carrillo-Moreno, D., Pressure and pressure derivative transient analysis without type-curve matching for elongated reservoirs with changes in permeability or width. CT&F – Ciencia, Tecnología y Futuro. 4(1), pp. 75-88, 2010.

[9]   Escobar, F.H. Recent advances in practical applied well test analysis. Nova publishers, New York. Published by Nova Science Publishers, Inc. † New York, 2015.

[10]   Foster, G.A., Wong, D.W., Asgarpour, S. and Cinco-Ley, H., Interference test analysis in limited reservoirs using the pressure derivative approach: Field example. Petroleum Society of Canada. January 1, 1994. DOI: 10.2118/94-30.

[11]   Jacob, C.E., On the flow of water in an elastic artesian aquifer. American Geophysical Union 21, pp. 574-588. 1940. DOI: 10.1029/TR021i002p00574.

[12]   Kamal, M.M., Interference and pulse testing-A review. Journal of Petroleum Technology, Society of Petroleum Engineers. 35(12), pp. 2257-2270, 1983. DOI: 10.2118/10042-PA.

[13]   Martinez, N.R. and Samaniego, F.V., Advances in the analysis of pressure interference tests. Journal of Canadian Petroleum Technology Society of Petroleum Engineers, 49(12), pp. 65-70, 2010. DOI: 10.2118/141028-PA.

[14]   Martinez, J.A., Escobar, F.H. and Cantillo, J.H., Application of the TDS technique to dilatant Non-Newtonian/Newtonian Fluid composite reservoirs. Ingeniería e Investigación Journal. 31(3), pp. 130-134, 2011. DOI: 10.15446/ing.investig

[15]   Matthies, E.P., Practical application of interference tests. Journal of Petroleum Technology, Society of Petroleum Engineers, 16(03), pp. 1-4, 1964. DOI: 10.2118/627-PA.

[16]   Miller, F.G., Theory of unsteady-State influx of water in linear reservoirs. Journal Institute of Petroleum 48(467), pp. 365-379, 1962.

[17]   Ouandlous, A., Interpretation of interference test by Tiab's direct synthesis technique, MSc. Thesis. University of Oklahoma, United States, 1999.

[18]   Tiab, D. and Kumar, A., Application of the P'D function to interference analysis. Society of Petroleum Engineers, 1980. DOI: 10.2118/6053-PA.

[19]   Tiab, D., Analysis of pressure and pressure derivative without type-curve matching: 1- Skin and wellbore storage, Journal of Petroleum Science and Engineering, 12(3), pp. 171-181, 1995. DOI: 10.1016/0920-4105(94)00040-B.

F.H. Escobar-Macualo, received the BSc. in 1989 from Universidad de América, Bogotá, Colombia, the MSc. (1995) and PhD (2002) degrees in Petroleum Eng. from the University of Oklahoma. All his degrees are in Petroleum Eng. He is the director of the GIPE Group in Universidad Surcolombiana where has been a professor since 1996. He has also worked as a consultant for several oil and service companies. He has published more than 150 papers, four research books and three book chapters.
ORCID: 0000-0003-4901-6057

E. Rojas-Borrego, received the BSc. Petroleum Eng. in 2017. Member of the GIPE Group in Universidad Surcolombiana.
ORCID: 0000-0002-2681-2432.

N.T. Alarcón-Olaya, received the BSc. Petroleum Eng. in 2017. Member of the GIPE Group in Universidad Surcolombiana.
ORCID: 0000-0002-4000-3156.

Nomenclature

b	Reservoir width, ft
B	Oil volume factor, RB/STB
c_t	Total compressibility, 1/psi
h	Formation thickness, ft
h_D	Formation thickness and wellbore radius ratio (assuming isotropy), (h/r_w)
L	Linear distance between wells, ft
$m(P)$	Pseudopressure, psi²/cp
P	Pressure, psi
P_D	Dimensionless pressure
q	Oil flow rate, BPD
q_g	Gas flow rate, Mscf/D
r	Radial distance, ft
r_D	Dimensionless radius, (r/r_w)
r_w	Wellbore radius, ft
s	Skin factor
t	Time, hr
T	Temperature, °R
t_D	Dimensionless time based on wellbore radius
t_{DA}	Dimensionless time based on drainage area
$t_a(P)$	Pseudotime, hr-cp/psi
t_{Da}	Dimensionless pseudotime
$t*\Delta P'$	Pressure derivative, psi
t_D*P_D'	Dimensionless pressure derivative
x	Linear distance from observation well to reservoir, ft
x_D	Ratio of linear distance and well distance, (x/L)

Suffixes

D	Dimensionless
i	Intercept, initial
L	Linear
$L1$	Linear at 1 hr
Li	Intercept of pressure and pressure derivative curves for linear case
pss	Pseudosteady state
$pss1$	Pseudosteady state at 1 hr
sph	Spherical
$Sph1$	Spherical at 1 hr
$sphi$	Intercept of pressure and pressure derivative curves for spherical case
SS	Steady state
$SS1$	Steady state at 1 hr
w	well

Greek

Δ	Change, drop
α_L	887.2
α_{sph}	70.6
β	0.0002637
η	Diffusivity constant
ϕ	Porosity
μ	Viscosity, cp

Appendix A. Gas flow Equations

[1] introduced the pseudotime function to account for the time dependence of both gas viscosity and total system compressibility:

$$t_a = \int_{to}^{t} \frac{dt}{\mu(t)c_t(t)} \tag{1}$$

This function is better defined as a pressure function given in hr psi/cp:

$$t_a(P) = \int_{Po}^{P} \frac{(dt/dP)}{\mu(p)c_t(P)} dP \tag{A.2}$$

Now, μ and c_t are pressure dependent properties. Rewriting Eq. (3) can be rewritten as:

$$t_D = \frac{0.0002637\overline{k}t}{\phi(\mu c_t)_i r_w^2} \tag{A.3}$$

Including the pseudotime function, $t_a(P)$, in Eq. (A.3), the dimensionless pseudotime is given by:

$$t_{Da} = \left(\frac{0.0002637k}{\phi r_w^2}\right) t_a(P) \tag{A.4}$$

Multiplying and, then, dividing by $(\mu c_t)_i$ a similar equation to the general dimensionless time expression;

$$t_{Da} = \left(\frac{0.0002637k}{\phi(\mu c_t)_i r_w^2}\right)\left[(\mu c_t)_i \times t_a(P)\right] \tag{A.5}$$

The dimensionless pseudopressure and pseudopressure derivative are defined by:

$$m(P)_D = \frac{kh[m(P_i) - m(P)]}{1422.52 q_g T} \tag{A.6}$$

$$t_D * m(P)'_D = \frac{kh[t*\Delta m(P)']}{1422.52 q_g T} \tag{A.7}$$

For gas linear flow regime interference, Eqs. (7), (9) and (12) become:

$$\phi = \frac{k(t_a(P))_{Li}}{15239024 \ r_w^2}\left(\frac{x}{L}\right)^{4.32} \frac{1}{b^{4.14}} \tag{A.8}$$

$$k = \frac{5955223 x^{2.062} q_g T}{L^{2.7333} h\left[m(P_i) - m(P)\right]_L} \tag{A.9}$$

$$k = 12492596\left(\frac{(t_a(P))_L}{\phi r_w^2}\right)^{0.3844}\left(\frac{q_g T}{h[t*\Delta m(P)']_L}\right)^{1.3844} \frac{x^{4.5159}}{L^{5.4453} b^{1.5921}} \tag{A.10}$$

For spherical gas flow regime interference, Eqs. (18), (20) and (22) become:

$$\phi = \frac{1.5\times10^{-3} k(t_a(P))_{sphi} h^{0.5} r_w^{0.2}}{r^{2.7}} \tag{A.11}$$

$$k = \frac{41.4850 \ q_g T}{h\left[m(P_i) - m(P)\right]_{sph}} \left(\frac{r}{r_w}\right)^{0.3} \qquad (A.12)$$

$$k = \frac{153.45 r^{1.1}}{h^{0.8334} r_w^{0.2667}} \left[\frac{\phi}{(t_a(P))_{sph}}\right]^{0.3333} \left[\frac{q_g T}{\left[t * \Delta m(P)'\right]_{sph}}\right]^{0.6667} \qquad (A.13)$$

For late time behavior, Eqs. (26), (28), (30), and (32) become:

$$A = \frac{2.4253 q_g T (t_a(P))_{pss}}{\phi h [t * \Delta m(P)']_{pss}} \qquad (A.14)$$

$$A = \frac{2.4837 q_g T (t_a(P))_{pss}}{\phi h [t * \Delta m(P)']_{pss}} \qquad (A.15)$$

$$A = \frac{k^2 h (t_a(P))_{SS} [t * \Delta m(P)']_{SS}}{2870475 q_g \phi T} \qquad (A.16)$$

$$A = \frac{k^2 h (t_a(P))_{SS} [t * \Delta m(P)']_{SS}}{85542164 q_g \phi T} \qquad (A.17)$$

UNIVERSIDAD **NACIONAL** DE COLOMBIA

SEDE MEDELLÍN

FACULTAD DE MINAS

Área Curricular de Ingeniería
Química e Ingeniería de Petróleos

Oferta de Posgrados

Maestría en Ingeniería - Ingeniería Química
Maestría en Ingeniería - Ingeniería de Petróleos
Doctorado en Ingeniería - Sistemas Energéticos

Mayor información:

E-mail: qcaypet_med@unal.edu.co
Teléfono: (57-4) 425 5317